Final Report

NASA NAG5-3231

Supplement to "Spectral Models of Neutron Star Magnetospheres"
Term: 11/15/95 - 11/14/96

PI: Roger W. Romani
Department of Physics, Stanford University

This grant has a somewhat complicated history. The award was an approved subcontract under James M. Cordes' *CGRO* grant "OSSE and EGRET Observations of Known and New Pulsars". Eventually the funds were transmitted as a supplement to my NASA Theory Program Grant "Spectral Models of Neutron Star Magnetospheres" (NAG5-3101), but were then re-issued as an independent *CGRO* contract. Our contribution towards Cordes' program was to model high energy pulsar light curves, produce new intermediate energy models for any OSSE detections and to suggest candidates for future searches. The goal of these researches was to characterize the high energy beaming patterns and luminosity functions of these pulsars as a class and to investigate their galactic population.

Because of the limited OSSE sensitivity, no new pulsars were detected under this program. However, the funds at Stanford supported graduate student research that resulted in improved models for the pulsar light curves and improved estimates for the local high energy pulsar population. These results have been reported in Yadigaroglu and Romani (1997, ApJ in press). Preprints of this work are enclosed.

The spectral modeling program (NAG5-3101) is continuing through 10/97. We anticipate that a more complete paper on the physics of the X-ray through gamma-ray emission will be submitted during this period. Work on detailed numerical models is underway and progress will be reported at the upcoming Compton GRO Symposium.

γ-Ray Pulsars and Massive Stars in the Solar Neighborhood

I.-A. Yadigaroglu and Roger W. Romani[1]
Department of Physics, Stanford University, Stanford, CA 94305-4060

ABSTRACT

We revisit the association of unidentified Galactic plane *EGRET* sources with tracers of recent massive star formation and death. Up-to-date catalogs of OB associations, SNRs, young pulsars, HII regions and young open clusters were used in finding counterparts for a recent list of *EGRET* sources. It has been argued for some time that *EGRET* source positions are correlated with SNRs and OB associations as a class; we extend such analyses by finding additional counterparts and assessing the probability of individual source identifications. Among the several scenarios relating *EGRET* sources to massive stars, we focus on young neutron stars as the origin of the γ-ray emission. The characteristics of the candidate identifications are compared to the known γ-ray pulsar sample and to detailed Galactic population syntheses using our outer gap pulsar model of γ-ray emission. Both the spatial distribution and luminosity function of the candidates are in good agreement with the model predictions; we infer that young pulsars can account for the bulk of the excess low latitude *EGRET* sources. We show that with this identification, the γ-ray point sources provide an important new window into the history of recent massive star death in the solar neighborhood.

Subject headings: pulsars — gamma rays — HII regions — OB associations — SNRs

1. Introduction

At least two distinct populations of sources have been detected above 100 MeV by the *EGRET* experiment on *CGRO*: extragalactic AGN, and a population of $\sim$ 30 Galactic sources with small scale height. Five of the Galactic sources have now been identified from their pulsations as newly born neutron stars. It has been known for some time (Lamb 1978, Montmerle 1979) that the Galactic population is, *as a class*, closely linked with young objects. Montmerle showed that about half of the 11 unidentified Galactic *COS B* sources could be associated with "SNOBs," spatial coincidences between SNRs and OB associations (or HII regions as their tracers). Conversely, as many as three-fourths of the best identified SNOBs were seen in γ rays. However, SNRs as a class were clearly not all γ-ray emitters. In principle γ rays from the SNOBs could be due to any combination of features of young regions, and the particular scenario advanced by Montmerle was that the dense neighborhoods of massive star associations act as targets for the cosmic rays produced in shock waves of SNRs, resulting in γ rays from π^0 decay.

Surprisingly, even though two of the brightest sources had already been identified with the Crab and Vela pulsars, it was not proposed that the other sources are also young isolated pulsars. Since then, the γ-ray source positions have of course been extensively searched for radio pulsations, and, conversely, the known young radio pulsars have been searched for γ rays (see Thompson 1994 for recent upper limits). Only three new pulsars with both radio and γ-ray emission have been found in this manner (PSRs B1706-44, B1055-52 and B1951+32). Even though it is notoriously difficult to detect short period radio pulsars in the dense interstellar medium of massive star forming regions, the small number of identifications would seem to cast doubt on pulsars as the origin of all Galactic γ-ray sources. However, the discovery of the Geminga γ-ray pulsar from its X-ray pulsations (Halpern and Holt 1992) has dramatically altered our picture of the γ-ray pulsar population, as it presents no observed radio emission. Several authors have thus recently revisited the question of whether all the unidentified γ-ray sources are in fact isolated neutron stars waiting to be discovered as such.

Duplication of the discovery in X-rays of the Geminga pulsar to other sources has proven difficult, and direct searches of pulsations in γ rays have only recently begun to place limits on the pulsed fraction and spin parameters of the brightest few sources (Mattox *et al.* 1996). Until more high energy data becomes available population studies are thus an interesting alternative in exploring the nature of the unidentified sources.

[1]Alfred P. Sloan Fellow

Halpern and Ruderman (1993) and Helfand (1994) assume simple forms for the evolution with age of the efficiency η_γ of conversion of spin-down power to γ rays and single values for the beaming fraction f_γ of γ rays on the sky and conclude that all γ-ray sources may well be pulsars. Mukherjee *et al.* (1995) arrive at the opposite conclusion by estimating the distance and luminosity of the unidentified *EGRET* sources from their distribution in Galactic longitude and latitude. Assuming again a unique value for f_γ, they find that luminosities of the unidentified sources are too large to be Geminga-like objects. In Romani and Yadigaroglu (1995, RY) we presented an outer gap model for the emission of high energy γ rays by pulsars younger than a million years. In our model both η_γ and f_γ evolve with pulsar age, and the beaming pattern differs from that of the radio emission. Monte Carlo sums (Yadigaroglu and Romani 1995, YR) showed that most of the unidentified *EGRET* sources are expected to be Geminga-like pulsars with no detectable radio emission. Other pulsar γ-ray emission models, such as the extended polar cap models of Daugherty and Harding (1996) and Sturner and Dermer (1996), predict that at most a few of the unidentified sources are pulsars, many of which should have faint radio emission.

Kaaret and Cottam (1996, KC96) have recently revisited Montmerle's hypothesis. They find that 16 of 25 unidentified *EGRET* sources lie in or near OB associations, with a probability that the superposition as a class is due to chance of 10^{-4}. Several of the 16 sources are also noted to have coincident SNRs and/or radio pulsars. The authors estimate distances to the *EGRET* sources from the association distances, and construct an intrinsic luminosity function. The luminosity function is found to be consistent with the known γ-ray pulsars, leading the authors to conclude that a majority of the *EGRET* unidentified sources are probably pulsars.

Sturner and Dermer (1995, SD95) have searched for coincidences between unidentified γ-ray sources and SNRs using a much improved test of association. Along with Esposito *et al.* (1994) they find a statistically significant correlation. All of the SNRs found to be coincident with *EGRET* sources are in fact SNOBs, and are present in the association lists of both Montmerle and KC96. The view adopted in SD95 is that the γ-ray emission originates from the remnants and three possible mechanisms are suggested: pulsar powered plerionic emission from filled-center SNRs, and for shell-type SNRs either non-thermal bremsstrahlung (from the synchrotron emitting electrons) or π^0 decay from remnant-generated cosmic rays colliding with the interstellar medium. Note that as in the SNOB hypothesis, the γ-ray sources should then be extended. To date this has only been tested for 2EG J2020+4026 (Brazier *et al.* 1996) which is unresolved, in contrast to the associated SNR γ Cygni.

We update these studies with an improved version of the test statistic of SD95 (§2), finding coincidences between the most recent *EGRET* source list and an up-to-date catalog of young region tracers, including OB associations, SNRs, young pulsars, HII regions, and young open clusters (§3). We present combined results for all types of objects, and construct a luminosity function for the sources from the estimated distances to the counterparts (§4). We then focus on young pulsars, and compare a Monte Carlo population synthesis (§5) using our outer gap model and a detailed model of the solar neighborhood with the luminosity function and other characteristics of the now "identified" sources (§6).

2. Test of Association

We have extended Sturner and Dermer's test of association between *EGRET* sources and SNRs to allow a general search for counterparts. Their statistic is $\alpha_1 = (r_1/r_2)^2$, where r_1 and r_2 are the angular distances from an unidentified source to the nearest and second nearest young object. Interpreting $2/r_2^2$ as an estimate of the local density of young objects n_y, α_1 will then be distributed uniformly between 0 and 1 for random populations, and small values of α_1 will indicate unlikely coincidences. The "1 σ confidence interval" on α_1 is simply $\sigma_{\alpha_1} = \pm\ 0.32$.

Sturner and Dermer's test has the advantage that it does not require an independent estimate of the local density of a given object class, as obtained for instance from CO maps (*cf.* KC96). Such estimates do not eliminate unknown observational biases intrinsic to the object catalogs. While keeping this useful property we have taken into account the angular size of the objects as well as errors in the determination of the source position.

We use the *EGRET* source location 2D Gaussian probability distribution and construct its overlap integral Q with a second 2D Gaussian distribution associated with each young object in our catalogs. For counterparts other than pulsars, the width of this second Gaussian is set to the object's angular size, s. The integral Q is thus the probability that the γ-ray source position is within the boundary of the object, with the object position weighted as a Gaussian about its nominal center.

The overlap integral is then normalized by the expected number of catalog sources within the *EGRET* error circle and the resulting ratio compared with the distribution of ratios expected for a random population of similar young objects at density n_y. As in SD95, n_y is estimated from nearest neighbors in the catalog (we have chosen to use the third nearest neighbor, since several catalog sources are typically within the scale of Galactic structures). So for each unidentified *EGRET* source, we find the nearest young object in a counterpart catalog, and report the probability P that a larger ratio would have been found by chance (P[Q, n_y] was obtained from Monte Carlo sums). For uncorrelated samples these probabilities are uniformly distributed, and with 35 *EGRET* sources, we should find one pair with P < 3 %. In fact since $\sim$ 10 sources have very small P, less than one pair is expected to have P < 3 % due to chance.

3. Object Catalogs

3.1. *EGRET* sources

The Second *EGRET* Catalog (Thompson *et al.* 1996) lists 71 unidentified γ-ray sources, 33 of which fall within $|b| < 10°$ of the Galactic plane. In finding associations, we have used the updated list of Thompson *et al.* 1996b. This list benefits from additional phase III exposure, and lists 8 additional sources with $|b| < 10°$. In our analysis we have eliminated sources for which the *average* flux in the three phases results in a significance $\sqrt{\mathrm{TS}}$ of less than 5 (approximately 5 σ, $\sqrt{\mathrm{TS}}$ as defined in Thompson *et al.* 1996), as this is the threshold used in modeling the *EGRET* sensitivity in section §5. The error ellipses for the source positions are given in Thompson *et al.* and their mean radius is $\sim 30'$. Uncertainties remain in understanding *EGRET* likelihood distributions, and a careful calculation using the detailed shape of the error contours instead of 2D Gaussians will clearly be of benefit to an update of the present counterpart search.

3.2. OB Associations and Young Clusters

For a catalog of OB associations, we follow KC96 in using the list of Mel'nik and Efremov (1995). The O and B-stars of Blaha and Humphreys (1989) are partitioned by Mel'nik and Efremov into 58 OB associations using a cluster analysis method. Of the 630 O-stars present in the star catalog, $\sim$ 75 % are found to lie in associations. For each OB association, the mean position, distance, size, and number of stars are given. The associations have a mean size of 40 pc and a mean distance of $\sim$ 1.6 kpc. Associations with size less than $\sim$ 15 pc are defined as young open clusters. We note that distances to O and B-stars are accurate to only $\sim$ 20 %.

It is well-known that large OB associations are complex and can often be partitioned further into sub-structures, see Garmany (1994) for a review. The algorithm of Mel'nik and Efremov finds these sub-structures and reports them as separate OB associations. In their nomenclature, these fragments will have the same group name with the added suffices A, B, C, etc. As we estimate the local density of OB associations for our test statistic from the distance to the third nearest unassociated neighbor, we ignore fragments from the same association in selecting nearest neighbors.

In addition to the four open clusters found by Mel'nik and Efremov we have used the 160 open clusters younger than $10^{7.5}$ years in the catalog of Janes, Duke and Lyngå (1987). The mean distance to the open clusters is $\sim$ 2.1 kpc.

3.3. HII regions

HII regions and their associated molecular clouds are convenient additional tracers of O and B-stars. The observational situation has not changed much since Montmerle's (1979) study, and we have also used Georgelin and Georgelin's (1976) catalog of 100 giant HII regions. Georgelin and Georgelin map the spiral structure of the Galaxy and thus select HII regions that would be prominent to an observer external to our Galaxy, so that their sample includes only intrinsically large and bright HII regions. Distance and class are reported in the tables of Georgelin and Georgelin. Region class reflects the radio size and brightness of the region and is one of 'f', 'm' or 'b'. For 40 of the 50 HII regions within 5 kpc, the region size could be determined from Maršálková (1974) and other original sources. For the distant radio selected regions, we have assumed a diameter of 50 pc. Many of the giant HII regions are complex associations of smaller HII regions.

Brand and Blitz (1993) have compiled a much more detailed but local sample of 206 kinematically distinct HII regions from various optically selected catalogs. The HII region sizes are not given in this catalog but were available from the original references in most cases. The mean distance of the local sample is $\sim$ 2.6 kpc. We do not expect to find good (small P) *EGRET* counterparts in the local sample of HII regions since it distinguishes between different sub-structures of the same large massive star forming region, skewing the test estimate of the local density of unassociated HII regions.

3.4. Young Radio Pulsars and SNRs

O and B-stars are the direct progenitors of neutron stars, and five *EGRET* sources are presently identified with radio pulsars: the Crab pulsar, Vela, PSRs B1706-44, B1055-52 and B1951+32, all younger than 10^6 years. Extensive γ-ray searches of all known radio pulsars have of course been performed (Thompson *et al.* 1994, Fierro 1996). For completeness and as a test of our statistic we have looked for associations between unidentified sources and young radio pulsars. An extensive catalog of radio pulsars is available from the Princeton Pulsar Group (see Taylor, Manchester and Lyne 1993) and contained 104 pulsars younger than 10^6 years at the time of our analysis.

The Princeton database is collated from many different radio surveys and thus has non-uniform flux limit. The pulsar sample has a mean distance of $\sim$ 6 kpc but is certainly not complete to this distance. There are strong selection effects for very young radio pulsars that bias the sample towards long periods and high magnetic fields. In addition radio pulsars are difficult to detect in regions of high electron density n_e, such as in complexes of SNRs, HII regions and O and B-stars.

SNRs generally persist for $\lesssim 10^5$ years and are ideal tracers of recent massive star death. We use the latest SNR catalog of Green (1995) containing 194 SNRs. SNR position and angular size were taken from the catalog, but we adopt distance determinations from HI absorption or Sedov solutions in the literature, when available. When no estimate was available, we compute the $\sigma - D$ distance which is notoriously inaccurate. In the near future more accurate Sedov X-ray distances should be available from the ROSAT all-sky survey, see Namir *et al.* (1994). The SNR sample is collected from many sources and has a mean

distance of $\sim$ 3 kpc. Many additional SNRs are expected from the ROSAT survey, which will result in a deeper sample.

4. Coincident Sources

The complete list of γ-ray sources and their candidate associations are summarized in Table 1. For each *EGRET* source, we list the source position, flux, and all catalog objects that are consistent with the source position, rejecting pairs for which Q < 10 % (i.e. for the given source size and *EGRET* error circle, association can be rejected at the 90 % level). The probability P (defined in §2) that the coincidence is due to chance is listed for each pair. We have high confidence in the identification of the *EGRET* source if at least one probability P is < 3 %. We distinguish between these "IDed" sources (bold type) and "overlaps" for which the P of all coincident objects are > 3 %. Unfortunately, when several young objects are clustered in the same region of the sky, as often occurs along tangents to the spiral arms, we cannot ID an *EGRET* source with a unique object even though the source is probably associated with the region as a whole. Some overlaps are thus likely to be real coincidences. When P > 10 % we do not list P, but only Q.

In Figure 1 we plot the cumulative distributions of the probabilities P of association. For uncorrelated samples these probabilities should be uniformly distributed and would follow the diagonal line. Clearly all but the young open cluster and local HII region samples present significant numbers of improbably close counterparts. The largest excess of counterparts is found for the OB associations, followed by SNRs. Thirteen *EGRET* sources have at least one P < 3 %, and 20 have P < 10 %. Of the remaining sources, 3 have overlapping objects with Q > 10 %, so that only 12 *EGRET* sources have no coincident objects at all in the examined catalogs.

Our test has of course recovered the five pulsed identifications with known pulsars with very high confidence (P < 0.01 %); PSR B1951+32 is too faint to be included in the catalog as an unpulsed source. These are not included in Figure 1 or Table 1. The Crab Nebula, Vela and PSR B1706-44 remnants (MSH 17-41) are also found with high confidence (P < 3 %). Only the Vela pulsar has an OB association (OB Vela 1A) consistent with its position. No other coincidences are found. This is not surprising given the difficulty in detecting radio pulsations from regions of high electron density n_e.

Comparing with previous results, we have found all 7 SNR counterparts reported in SD95 for *EGRET* sources still present in our source list. However, only three of the seven, SNRs IC 443, MSH 11-61A and γ Cygni result in source IDs, and the coincidence with SNR G312.4-0.4 is just above our ID cut of P < 3 %. We have also found all of the 15 OB counterparts reported in KC96 for *EGRET* sources in our list. Six of the 15 result in IDs (Gem 1, Car 1 F, Sgr 1 C, Sgr 1 B, and Cyg 1,8,9 twice), and 10 have P < 10 % (add Mon 1 B, Clust 3, Car 1 A, and Cyg 1,8,9 again). Seven of the OB counterparts are also coincident with a SNR.

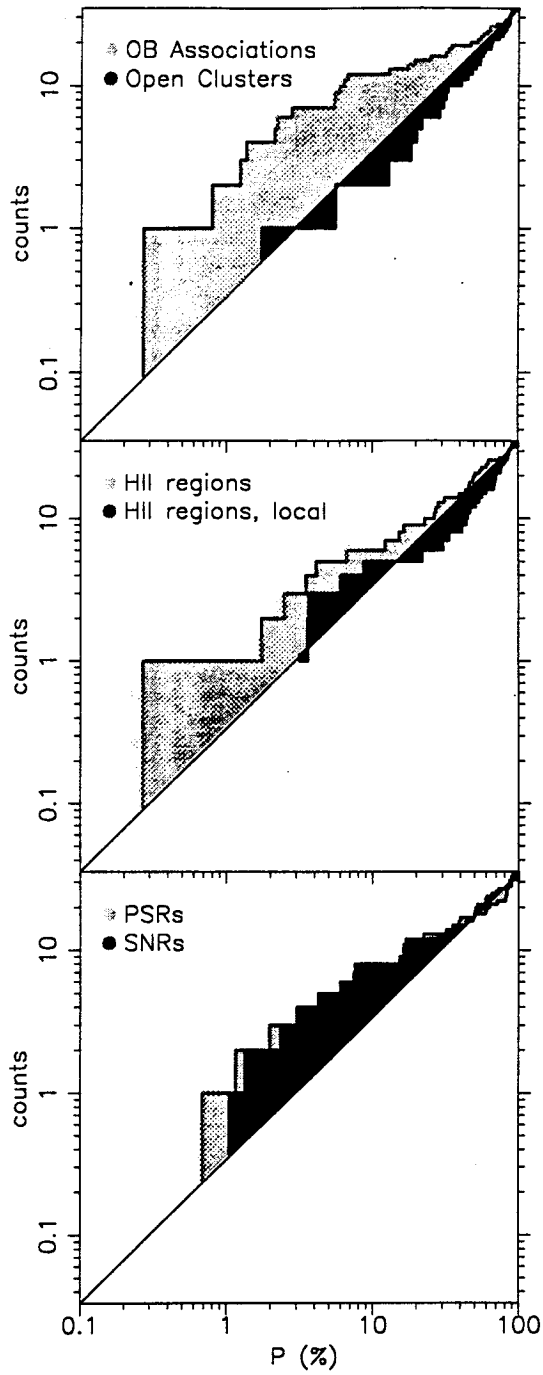

Fig. 1.— Cumulative distributions of association probabilities. The value P is the probability that an association pair is due to coincidence assuming uniformly distributed objects locally. The total number of unidentified sources is 35, so at each P we can expect 35 × P objects to have this value of P by chance if the pairs are unassociated; this value is denoted by the diagonal line. The shaded surface thus represents the excess number of associations.

For many of these *EGRET* sources, we have also found nearby HII regions. In addition we have seven new *EGRET* IDs or overlaps. Two of these are *EGRET* sources not present in earlier catalogs. No sources are IDed with an HII region from the local sample, as expected (see §3.3). Only one source is IDed with a young open cluster, Collinder 347. This indicates that neutron star formation ceased over a million years ago in most of the open clusters in our catalog.

Having found the list of γ-ray sources with candidate associations, we have assigned a distance d to each of the 23 IDs + overlaps. If a counterpart with P < 10 % was available, we chose the distance to the counterpart with smallest P. Otherwise we chose the distance to the counterpart with largest Q. The Galactic positions of these 22 sources along with the five known γ-ray pulsars are plotted in Figure 2. Note that when there are several counterparts for the same *EGRET* source it is often possible to identify a single distance with the entire complex.

We can now calculate the γ-ray luminosities for our candidate sources from the measured photon fluxes and estimated distances. The source spectra are often not well fit by a power law, and rather than assume a spectral index we have numerically summed the spectra above 100 MeV as given in Merck *et al.* (1996) (two of our IDed sources are not present in Merck's list and have not been included in the constructed luminosity function). An upper cutoff of 3 GeV was assumed when only upper limits on the high energy source flux were available. We have also assumed isotropic radiation ($f_\gamma = 1$). Typical isotropic luminosities are several $\times\ 10^{35}$ erg/s, similar luminosities have recently been inferred by KC96 and Kanbach *et al.* (1996). For pulsars in reality we expect f_γ as small as 0.1 in many cases (YR, R96); "isotropic" luminosities can therefore exceed the total spin-down power.

We note that pulsars would be expected to have indices of -1.7, but many may have an additional soft component due to plerionic emission or unresolved diffuse excesses from gas clumps or associated cosmic ray enhancement that will steepen the measured index. It is thus not surprising that Merck *et al.* find only a few spectral indices to show the characteristic hardness expected for pulsars. However, it is interesting that the handful of sources with hard spectra reported on in Merck *et al.* are independently singled out in our analysis as being good (low P) candidates.

5. Modeled Pulsar Population

We now turn to spin-down powered pulsars as the origin of the γ-ray emission. For the evolution of efficiency of spin-down power to γ rays we assumed in RY and YR a simple empirical law that matches the values for PSRs B1706-44 and B1055-52. A recently completed model of emission processes in the outer magnetosphere (Romani 1996, R96) gives a more complete description of the pulsar radiation. In R96 the efficiency of curvature radiation η_γ in the *EGRET* range is estimated as a function of age, magnetic field and inclination angle. The η_γ and f_γ laws of R96 thus allow a more accurate integration over an assumed population of young pulsars. The estimates of R96 are not applicable to very young pulsars such as the Crab, since the synchrotron flux important for these objects is not modeled in detail. We have chosen to increase η_γ over the curvature value of R96 by adding $\eta_{synch} = 10^{-3}\,(3/B_{12})\,(10^3/\tau)$ to approximate this extra flux. As noted in R96 this synchrotron flux will also contribute to gap closure, thus decreasing the curvature η_γ for short period pulsars.

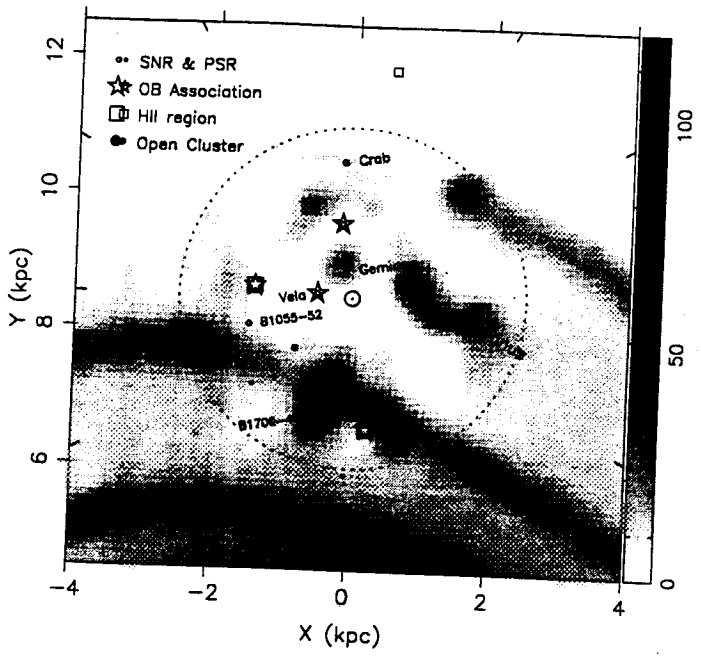

Fig. 2.— Distribution of candidates in the Galactic plane, viewed from directly above the Sun. Larger symbols are for young objects associated with an unidentified *EGRET* source with high probability (IDs), and smaller symbols for overlap candidates. The background gives the modeled distribution of O-stars. Shading is normalized to show the corresponding number of neutron stars per kpc^2 younger than 10^6 years (for a birth rate of 1/100 years). The radial tick marks are for Galactic l at 30° intervals, counterclockwise from the bottom.

We have computed populations over a range of parameters, but adopt standard pulsar properties (inferred from radio studies) for this discussion and the figures, and discuss the sensitivity of our results to these choices below. Our standard pulsar population is born at a rate $R = 1/100$ years at spin periods of 10 ms, with magnetic field distributed as a Gaussian in log B, with mean log B of 12.3 and dispersion 0.3, and with magnetic inclination α distributed isotropically at birth. We ignore any field evolution.

We have constructed a somewhat detailed model of the Galactic distribution of pulsars at birth, since both local

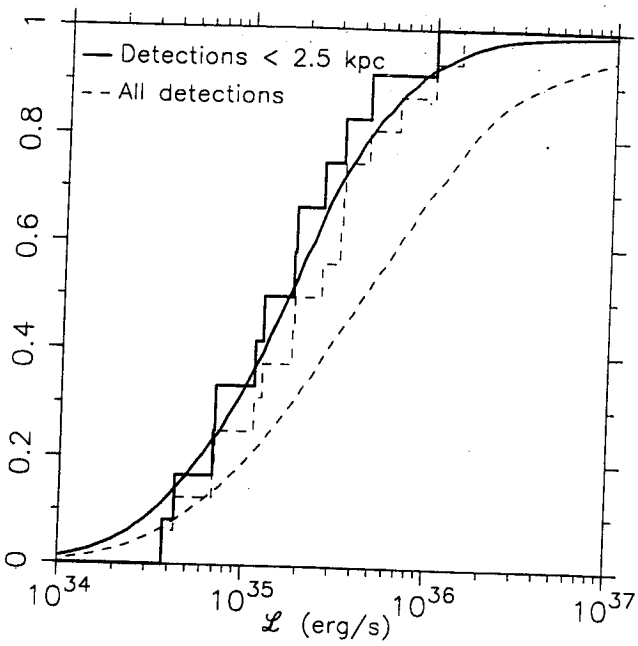

Fig. 3.— Luminosity functions for the IDed and modeled populations. Both complete and truncated (< 2.5 kpc) luminosity functions are shown. Only the truncated luminosity functions should be compared as the IDs are incomplete beyond 2.5 kpc.

and large-scale variations are important to the distribution of sources on the sky. For the large-scale structure, we begin with the free electron density model of Taylor and Cordes (1993) as a convenient tracer of the spiral arm and inner Galaxy structure. We add to these components a uniform density with the same radial dependence as the spiral arms: constant within 8.5 kpc of the Galactic Center, and falling off as $\mathrm{sech}^2((r - 8.5\ \mathrm{kpc})/2)$ beyond. The local density variations are given by the observed distribution of O-stars. For this purpose we created a model of the O-star population on a scale of 200 pc, smoothing the O-star density in the catalog of Garmany *et al.* (1982). We then normalized the large-scale model from the O-stars by summing all O-stars within 0.5 kpc of a spiral arm in the approximately complete sample within 2.5 kpc of the Sun. The resulting space density of O-stars normalizes the arm component over the same region; O-stars in the inter-arm region give the mean density of the uniform component. The local structure of the O-star distribution was then imposed using the smoothed catalog positions; this smooth map fades into the uniform background on a Gaussian scale length of 1.5 kpc. The resulting distribution is shown in Figure 2. This gives a reasonable picture of the large scale Galactic structure and the local texture in the density of massive star formation. We give pulsars generated from this map a Gaussian scale height at birth of $z_0 \sim 80$ pc and a Galactic z velocity drawn from the 1-D projection of the 2-D Lyne and Lorimer (1994) distribution.

A surprising result is that the density model thus constructed follows very closely on large scales the pulsar density model of Johnston (1994), obtained from radio pulsar studies alone, increasing our confidence as to the adequacy of our model on these scales. Locally, the Sun is found to be in a region of unusually low density; within a few kpc however, density is enhanced due to the Carina-Sagittarius arm. There are also smaller enhancements in the Orion spur and Cygnus directions, as well as at approximately 0.5 kpc in the anti-center direction.

For completeness and in order to discuss the effects of radio selection on our population studies, we also model the radio emission, which originates in a physically distinct region of the magnetosphere. We follow Johnston in modeling the radio emission and assume the beaming evolution of Biggs (1990):

$$W(\mathrm{P}) = 6.2^\circ\ \mathrm{P}^{-1/2},$$

and the radio luminosity law of Lorimer *et al.* (1993), in standard units of mJy kpc^2 at 400 MHz:

$$L_{400} = 2.8\ \mathrm{mJy\ kpc^2}\ \dot{\epsilon}^{1/2},$$

where $\dot{\epsilon}$ is the smaller of $\mathrm{P}\dot{\mathrm{P}}/10^{-15}$ and 10^2, with a Gaussian spread in $\log L_{400}$ of 0.8.

A Monte Carlo integration of the population then begins with draws of the pulsar properties: angle α, age t, field B, z_0 and v_z. We evolve the pulsar to its assumed age and calculate the derived parameters τ, P, $\dot{\mathrm{P}}$, B_{obs}, $\dot{\mathrm{E}}$, and z. We compute the correct γ-ray and radio luminosities and beaming factors for the pulsar parameters and determine the fraction of the sky that is swept out by the γ-ray and radio beams to find the detection probability and the maximum detectable distance at a given threshold.

The γ-ray threshold varies over the sky in Galactic l and b and is constructed from the *EGRET* background model and exposure map for phases I–III, scaled so as to conform to the catalog inclusion criterion of likelihood $\sqrt{\mathrm{TS}}$ greater than 5 ($\sim 5\ \sigma$). The resulting map consists of a single total photon flux sensitivity > 100 MeV at each location on the sky. The η_γ law of R96 results in a total energy flux from each pulsar, but not in a detailed prediction of the pulsar spectrum, which is ~ -1.7 depending on the pulsar age. We assume this spectrum with a cutoff at 3 GeV in converting the photon flux to a energy flux threshold. For comparison with other studies, this results in a mean threshold of 3×10^{-10} erg cm^{-2} s^{-1} when averaged over the Galactic plane.

We have not modeled the radio observations in detail, since selection effects on P that result in large observed magnetic fields for the young radio pulsar population are not adequately known. The effects of regions of massive star formation on the sensitivity of individual surveys is also poorly known. A simple radio flux threshold of 10 mJy approximates the average survey depth for the bulk of the young pulsar population.

Table 2: Expected Number of *EGRET* Detections

$\log\tau$ range	γ	γ + radio	γ < 2.5 kpc	γ + radio < 2.5 kpc
2.0 — 6.5	22.2	6.3	13.0	4.7
2.5 — 3.5	3.4	0.5	0.5	0.2
3.5 — 4.5	4.2	1.3	2.4	1.1
4.5 — 5.5	11.9	3.7	7.7	2.9
5.5 — 6.5	2.6	0.8	2.5	0.6

ID luminosity functions truncated at 2.5 kpc in Figure 3. The K-S test confirms that the truncated distributions are consistent. The histograms shown are for IDs including known sources. The luminosity function for the known sources only, or all sources (including overlaps) are both consistent with the luminosity function shown. Adding the effects of radio selection is not very important within our distance cut.

We now discuss the sensitivity of our results to modeling uncertainties. The mean isotropic luminosity of pulsars detected is not sensitive to the precise details of the population model, as pulsars of about the same flux tend to be selected at the *EGRET* γ-ray threshold. The upper end of the untruncated model luminosity function is dominated, however, by pulsars younger than 10^3 years seen at large distances, and is thus sensitive to the number of such objects detected. As noted at the beginning of section 5, very young pulsars were not modeled in detail. The spin and magnetic history of very young pulsars is also rather poorly constrained. For instance, doubling the initial spin period results in half as many detections of pulsars younger than 10^3 years. However, this has little effect on the truncated luminosity function as very few of these pulsars are detected within 2.5 kpc.

Varying the mean magnetic field within a reasonable range has again little effect on the mean luminosity of the detected sources. The total number of sources does change, increasing by 15 % when the mean log B is decreased to 12.2, and conversely when increased. Distributing the inclination angles α uniformly as opposed to isotropically ($\propto \sin\alpha$) as suggested by Gil and Han (1996) has essentially no effect.

7. Conclusions

As reported by Kaaret and Cottam, we find that the spatial distribution and luminosities of the low latitude *EGRET* sources are consistent with the proposition that most of the *EGRET* sources are pulsars. A modest admixture of a new class of Galactic *EGRET* sources with large scale height seems likely, and is hinted at in our l and b distributions. Allowing for a few such sources and the extragalactic AGN seen through the disk, we find that our outer gap model of γ-ray emission successfully matches the number and distribution of the bulk of *EGRET* Galactic plane sources.

We have also confirmed the striking result of Montmerle that virtually all of the *unidentified EGRET* sources with a coincident SNR are SNOBs, i.e. are also coincident with an OB association or HII region (with the possible exceptions of G359.0-0.9 and G312.4-0.4). We discuss this point further.

It is well known (Garmany 1994) that a large fraction of massive stars are found outside of OB associations. The ratio of "field" stars to those in associations increases with later spectral type, varying from ~ 0.2 for the most massive stars, to > 1 for stars later than B1, as determined from our catalog of massive stars. Runaway O-stars from associations can realistically account for only a small fraction of the field population, and so some isolated O-stars are formed in lower density regions of the Galaxy. We should therefore expect to find new-born pulsars in these same regions. In fact, if neutron stars are still being formed from stars later than B3, we would expect to find most pulsars outside of OB associations.

Of the known pulsars, only Vela is coincident with an OB association. Of our 8 IDs within 2.5 kpc of the Sun, 7 are coincident with an OB association. We thus find that 8 sources are within OB associations, and 5 are field pulsars. In essence, this explains Montmerle's discovery that the new γ-ray SNRs were SNOBs; in the solar neighborhood the bright pulsars outside of OB associations had mostly been detected as radio objects while those *within* OBs were still largely unidentified. Furthermore, many remnants outside of associations will likely be the product of Type Ia explosions leaving no neutron star. If pulsars are responsible for γ-ray production, this ensures that the sample of SNR counterparts is biased towards those in OB associations.

We note that our present counterpart sample already provides a lower limit on the mass of the stars which can form pulsars. The ~ 40 % field star fraction found for the known pulsars and IDs in the 2.5 kpc Solar neighborhood corresponds to a mean spectral class $\sim$ B1. With a steep IMF, the cut-off mass for neutron star formation could not then be lower than 13 $M_\odot$. This limit is presently still uncertain, for example assigning Poisson errors to the number of objects allows progenitor masses as low as 8 $M_\odot$. However, as explained in §6 we suspect that at least a few of the overlaps with OB associations are likely to be real, so that the fraction of pulsars found in OB associations would be even larger, and our cutoff mass higher. In fact, if all overlap candidates are real as suggested in KC96, then the field fraction drops to 30 % and the implied minimum mass for neutron star formation is 17 $M_\odot$. This exacerbates the well known problem in reconciling birth rates of pulsars with massive stars. Further refinements of this analysis, including improved estimates for the *EGRET* source positions and a more detailed treatment of the displacements between birth sites and parent OBs (*eg.* Geminga, rejected as coincident with an OB association may, in fact, be a runaway from the Orion OB 1 association: Frisch 1993;

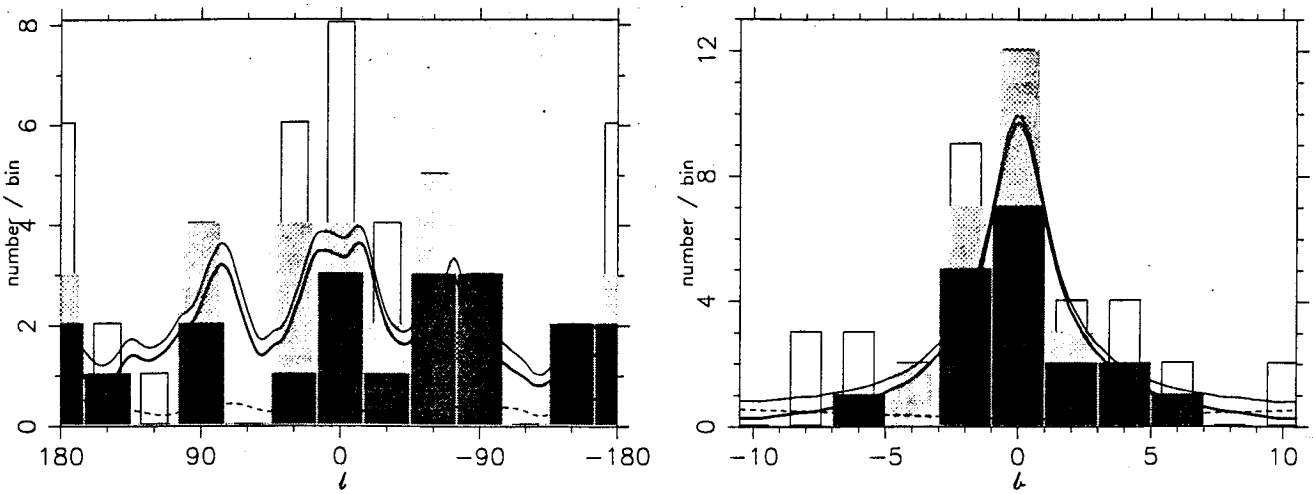

Fig. 4.— Distribution of candidates in Galactic longitude l and latitude b. Histograms from darkest to lightest are for Galactic *EGRET* source IDs (including the known pulsars), sources with overlap candidates, and sources with no association (outlined only). Lower dashed curve shows the expected number of AGN seen through the Galactic disk, upper dark curve is model prediction for the number of pulsars at a birth rate of 1/100 years, and the light curve is the sum of model + AGN.

6. Modeling Results

The expected numbers of detections for the f_γ and η_γ laws of R96 and our assumed pulsar population and detection thresholds are given in Table 2 as a function of age. Most detected pulsars have ages $\tau \sim 10^5$ years (somewhat older than in YR due to the improved η_γ law of R96). As in YR only a small fraction (< 30 %) of the γ-ray objects should also be detected as radio pulsars, although a few more might be detected in very deep searches at high DM.

As the Galaxy is transparent to γ rays, an unknown number of AGN must be taken into account in discussing our list of *EGRET* pulsar candidates. From the high latitude source sample Özel and Thompson (1996) have fit a simple power law to the AGN average flux distribution. Summing this law over the *EGRET* threshold map we find that a total of 4-6 sources within $|b| < 10°$ are probably AGN. Detailed analyses of the intermediate and high latitude *EGRET* sources (Grenier 1995, Özel and Thompson 1996, Nolan 1997) hint at the existence of a third class of Galactic *EGRET* sources with large scale height. A small number ~ 4 of the $|b| < 10°$ sources could belong to this third class. A few sources may be chance fluctuations in the background model and statistics. Since we have found 13 high confidence IDs as well as an additional 10 overlaps, the *EGRET* sources are in principle accounted for.

From Table 2 our model predicts ~ 22 detections in the *EGRET* range for $R = 1/100$ years. If all 10 of the overlaps were true associations, these together with the five known γ-ray pulsars and the 13 IDs would make 28 pulsars in the present *EGRET* sample —somewhat larger than predicted by our assumed birth rate. However, truncating the candidate population at the 2.5 kpc "completeness depth," still leaves 19 sources, whereas we expect only 13 sources from our model. Our counterpart catalogs are incomplete beyond 2.5 kpc so that we cannot expect to have associated all *EGRET* sources correctly, and from the numbers we would then conclude that many of the overlap candidates are chance superpositions of large nearby sources; i.e. the true counterparts lie further from the Sun than the characteristic catalog depth. A more likely explanation is that we have slightly overestimated the *EGRET* sensitivity and underestimated the local birth rate, so that several of the nearby overlaps are in fact true identifications.

We can compare the Galactic distributions in l and b of the candidate and modeled populations. This is shown in Figure 4. The model curves match the candidate distributions successfully, both in l and b (at a birth rate of 1/75 years the total number of sources, 40, is the same as observed, and the Poisson probability of both the observed l and b distributions is greater than 50 %). The density structures associated with the spiral arms and local variations are clearly identified in the l distribution, although some of the variation, *eg.* the large expected AGN density at $l \sim 180°$, are explained by variations in the *EGRET* survey sensitivity. The scale height and estimated distances of *EGRET* sources are consistent with our modeled population, as seen from the b distribution. As expected, no counterparts are found near $|b| \sim 10°$. It is interesting to note that *EGRET* sources with no counterparts have $|b| > 2°$ and tend to lie in the direction of the Galactic center $l \sim 0°$, hinting again at the existence of a third class of Galactic *EGRET* sources.

As described in §4, we have constructed a luminosity function for the IDs using the distances of the coincident young objects. As we are unlikely to have associated correctly sources beyond 2.5 kpc, we compare the model and

TABLE 1

UNIDENTIFIED *EGRET* γ-RAY SOURCES AND COINCIDENT YOUNG OBJECTS

Source	l (°)	b (°)	flux[a]	Candidate	P (%)	Q (%)	offset (°)	s (°)	d (pc)
2EG J0241+6119	135.7	1.2	105.7	HII S 199, IC 1848	**2.5**		1.8	2.0	**2300**
				HII[b]S 190		26	2.0	2.5	2100
				HII S 190, IC 1805		26	2.0	2.5	2300
				OB Cas 6		10	1.1	1.0	2010
2EG J0506+3424	170.8	-3.8	13.1	HII S 236, IC 410	6.6		3.4	0.9	**3400**
2EG J0511+5523	154.4	9.3	19.7						
2EG J0520+2626	179.0	-6.1	20.1						
2EG J0521+2206	182.9	-8.2	22.1						
2EG J0545+3943	170.8	5.7	15.1						
2EG J0618+2234	189.1	3.2	51.2	SNR IC 443, 3C157	**0.1**		0.2	0.8	**1100**
				OB Gem 1	**0.3**		0.4	1.9	1340
				PSR B0611+22	**3.0**		0.9	0.0	4720
				HII[b]S 249		18	1.2	1.3	1600
2EG J0635+0521	206.3	-1.2	21.3	HII S 275	**0.3**		0.9	1.7	**1500**
				OB Mon 1 B	5.9		0.8	0.6	1480
				HII[b]S 275	6.0		0.9	1.7	1600
				SNR Monoceros Neb		60	1.9	3.7	1200
				OB Mon 2 A		23	0.9	0.8	1630
2EGS J0852-4343	264.3	0.5	43.0	OB Vela 1 B	**2.8**		2.2	1.0	**1410**
				SNR Vela		21	3.8	4.2	500
				HII[b]BBW 192 D		16	1.6	1.5	1200
				HII[b]BBW 182		12	0.9	0.0	2120
2EG J1021-5835	284.4	-1.2	87.7	SNR MSH 10-53	**2.4**		0.6	0.4	**3800**
				OB Car 1 A	5.4		1.2	0.8	2400
				HII RCW 53, η Carina		37	3.2	4.5	2600
				HII RCW 49		37	0.9	1.2	4700
				HII G&G 55		22	0.5	f	5400
2EG J1049-5847	287.6	0.4	59.7	PSR B1046-58	**0.7**		0.3	0.0	**2980**
				OB Car 1 F	**2.2**		0.5	0.6	2760
				HII RCW 53, η Carina		85	1.3	4.5	2600
				OB Car 1 E		38	1.1	1.6	2640
				OB Car 1 B		12	1.6	1.6	2140
2EG J1103-6106	290.3	-0.9	56.3	SNR MSH 11-61A	**1.1**		0.2	0.2	**1900**
				PSR B1112-60	9.0		1.3	0.0	30000
				OB Car 2		83	0.8	2.5	2160
				HII RCW 57, G 38a		70	0.9	2.2	2500
				HII RCW 53, η Carina		48	2.7	4.5	2600
				HII G 35, H 43		40	0.6	0.5	7900
2EG J1412-6211	312.3	-0.8	90.5	SNR G 312.4-0.4	4.2		0.4	0.6	**1900**
2EGS J1418-6049	313.3	0.3	59.4	Cl Lyngå 2	5.5		0.9	0.2	**1100**
				OB Clust 3	6.7		0.3	0.8	1510
2EG J1648-5042	335.9	-3.7	40.9	HII RCW 108, G 53		36	2.2	3.0	**1300**
2EGS J1653-4604	340.1	-1.4	49.2						
2EGS J1736-2904	358.8	1.7	44.4						
2EG J1742-2250	4.8	3.9	35.3						
2EG J1746-0935	16.8	9.8	25.0						

Smith, Cunha and Plez 1994) give promise in resolving these questions. In particular, offsets from SNR positions due to the product neutron star velocity would strongly support the identification of the γ-ray sources with pulsar radiation; present positions are however too uncertain to effect this test.

We conclude in remarking that young radio-selected pulsars are clearly a strongly biased sample, weighted both towards long spin periods and regions free of large dispersion and electron scattering. To some extent, the present association of *EGRET* sources with sites of massive star formation selects pulsar candidates with opposite biases (large spin-down power $\dot{E}$ corresponds to short periods P, while proximity to massive stars results in large n_e). Thus the γ-ray selected pulsar sample gives a complementary view of the young pulsar population and a more representative census of the recent demise of massive stars in the Solar neighborhood.

Support for this work was provided by NASA grants NAG5-3101 and NAGW-4526. We thank Phil Kaaret for an early description of the work on OB counterparts, Thierry Montmerle for a detailed review of the manuscript and Joe Fierro, John Mattox, William Tompkins and Dave Thompson for discussion of *EGRET* source positions.

REFERENCES

Biggs, J.D. 1990, MNRAS, 245, 514
Blaha, C. and Humphreys, R. 1989, AJ, 98, 1598
Brand, J and Blitz, L. 1993, A&A, 275, 67
Brazier, K.T.S. *et al.* 1996, MNRAS, submitted
Daugherty, J. and Harding, A.K. 1996, ApJ, in press
Esposito, J.A. *et al.* 1994, BAAS, 26, 970
Fierro, J.M. 1996, Doctoral Thesis, Stanford University
Frisch, P.C. 1993, Nature, 364, 395
Garmany, C.D. *et al.* 1982, "A Catalog of Galactic O-Type Stars," (http://heasarch.gsfc.nasa.gov)
Garmany, C.D. 1994, PASP, 106, 25
Georgelin, Y.M. and Georgelin, Y.P 1976, A&A, 49, 57
Gil, J.A. and Han, J.L. 1996, ApJ, 458, 265
Green D.A., 1995, "A Catalog of Galactic Supernova Remnants (1995 July version)," Mullard Radio Astronomy Observatory, Cambridge, United Kingdom
Grenier, I.A. 1995, Adv. Space Res., 15, 73
Halpern, J.P. and Ruderman, M. 1993, ApJ, 415, 286
Halpern, J.P. and Holt, S.S. 1992, Nature, 357, 222
Helfand, D.J. 1994, MNRAS, 267, 490
Janes, K., Duke, C. and Lyngå, G. 1987, "A Catalog of Open Cluster Data," (http://heasarch.gsfc.nasa.gov)
Johnston, S. 1994, MNRAS, 268, 595
Kaaret, P. and Cottam, J. 1996, ApJ, 462, L1 (KC96)
Kanbach, G. *et al.* 1996, A&A, submitted
Lamb, R.C. 1978, Nature, 272, 429
Lorimer, D.R. *et al.* 1993, MNRAS, 263, 403
Lyne, A.G. and Lorimer, D.R. 1994, Nature, 369, 127
Mattox, J.R. *et al.* 1996, A&A, submitted
Merck, M. *et al.* 1996, A&A, submitted
Mel'nik, A.M. and Efremov, Yu.N. 1995, Astron. Let., 21, 10
Montmerle, T. 1979, ApJ, 231, 95
Maršálková, P. 1974, Ap&SS, 27, 3
Mukherjee, R. *et al.* 1995, ApJ, 441, L61
Namir, E.K. *et al.* 1994, ApJ, 427 L95
Nolan, P.L. 1997, in preparation
Özel, M.E. and Thompson, D.J. 1996, ApJ, 463, 105
Romani, R.W. 1996, ApJ, in press (R96)
Romani, R.W. and Yadigaroglu, I.-A. 1995, ApJ, 438, 314 (RY)
Smith, V.V., Cunha, K., and Plez, B. 1994, A&A, 281, L41
Sturner, S.J. and Dermer, C.D. 1996, ApJ, 461, 872
Sturner, S.J. and Dermer, C.D. 1995, A&A, 293, L17 (SD95)
Taylor, J.H. and Cordes, J.M. 1993, ApJ, 411, 674
Taylor, J.H., Manchester, R.N., and Lyne, A.G. 1993, ApJS, 88, 529 (http://pulsar.princeton.edu)
Thompson, D.J., *et al.* 1996b, ApJS, submitted
Thompson, D.J., *et al.* 1996, ApJS, 101, 259
Thompson, D.J., *et al.* 1994, ApJ, 436, 229
Yadigaroglu, I.-A. and Romani, R.W. 1995, ApJ, 449, 211 (YR)

This 2-column preprint was prepared with the AAS LaTeX macros v4.0.

TABLE 1—*Continued*

Source	l (°)	b (°)	flux[a]	Candidate	P (%)	Q (%)	offset (°)	s (°)	d (pc)
2EG J1746-2852	0.2	-0.1	110.9	Cl Collinder 347	**1.7**		0.4	0.1	**1500**
2EG J1747-3039	358.8	-1.3	40.9	SNR G 359.0-0.9		11	0.5	0.4	**2600**
2EG J1801-2312	6.7	-0.1	55.1	PSR B1758-23	**1.2**		0.1	0.0	**3000**
				OB Sgr 1 C	**1.2**		0.7	0.8	1440
				HII M 20, RCW 147	3.5		0.3	0.3	2700
				HII[b] M 8	3.6		1.4	1.7	1800
				SNR W28	6.0		0.3	0.7	3000
				HII RCW 146, M 8		21	1.6	1.8	1500
2EG J1811-2339	7.5	-2.5	36.1	OB Sgr 1 B	**0.8**		0.5	0.3	**1940**
				HII[b] M 8	8.7		2.0	1.7	1800
				HII RCW 146, M 8		21	1.6	1.8	1500
2EG J1813-1229	17.5	2.5	54.8	HII S 54, RCW 167		48	1.4	2.2	**2200**
				HII[b] S 54		47	1.4	2.3	2000
				OB Ser 2		16	1.1	1.1	1450
2EG J1825-1307	18.4	-0.4	62.3	HII S 53, RCW 166	4.1		0.2	0.2	**4300**
				PSR B1823-13	8.4		0.5	0.0	4120
				HII S 54, RCW 167		16	2.1	2.2	2200
				OB Sct 3		16	1.1	1.2	1480
2EGS J1833-2754	6.0	-8.8	14.5						
2EG J1834-2138	11.8	-6.2	21.0						
2EG J1857+0118	34.8	-0.8	41.8	SNR W44, 3C392	7.4		0.4	0.5	**3300**
				PSR B1853+01	9.3		0.3	0.0	3300
				HII G&G 24		14	1.0	f	3000
2EGS J1903+0529	39.1	-0.1	45.3	PSR B1900+05	**2.0**		0.5	0.0	**3930**
				HII[b] S 74	3.2		1.4	0.1	2100
				SNR 3C396, HC 24	7.6		0.2	0.1	7700
				SNR G 40.5-0.5		17	1.4	0.4	3800
				SNR W50, SS433		16	2.0	1.5	5000
2EGS J1905-1120	24.4	-8.2	17.3						
2EG J2019+3719	75.5	0.6	82.3	HII G&G 33	**1.7**		0.4	f	**5700**
				OB Cyg 1, 8, 9	**2.1**		1.6	5.0	1370
				HII[b] S 104	3.6		0.7	0.1	4400
				HII S 109,108		89	4.6	18.3	1400
2EG J2020+4026	78.1	2.2	126.5	SNR DR4, γ Cygni	**1.4**		0.1	1.0	**1500**
				OB Cyg 1, 8, 9	**1.4**		1.5	5.0	1370
				HII S 109,108		95	2.8	18.3	1400
2EG J2026+3610	75.3	-1.2	46.8	OB Cyg 1, 8, 9	6.3		3.0	5.0	**1370**
				HII S 109,108		87	4.9	18.3	1400
2EG J2033+4112	80.2	0.7	82.4	OB Cyg 1, 8, 9	5.5		3.5	5.0	**1370**
				HII S 109,108		100	0.5	18.3	1400
2EG J2227+6122	106.6	3.1	49.2						

[a] *EGRET* photon flux $\times 10^{-8}$ cm^{-2} s^{-1} above 100 MeV.

[b] Local HII region sample.

NOTE.—PSRs B0611+22 and B1112-60 are not likely have been identified correctly since they have small values of $\dot{E}$ and are at large distances. 2EG-J1746-2852 is closest to SNR Sgr A East, thought to be near the Galactic center.